J. Am. Soc. Mass Spectrom. (2016) 27:1813–1823
DOI: 10.1007/s13361-016-1442-9

RESEARCH ARTICLE

Identification of the Phenol Functionality in Deprotonated Monomeric and Dimeric Lignin Degradation Products via Tandem Mass Spectrometry Based on Ion–Molecule Reactions with Diethylmethoxyborane

Hanyu Zhu, Joann P. Max, Christopher L. Marcum, Hao Luo, Mahdi M. Abu-Omar, Hilkka I. Kenttämaa

Department of Chemistry, Purdue University, West Lafayette, IN, USA

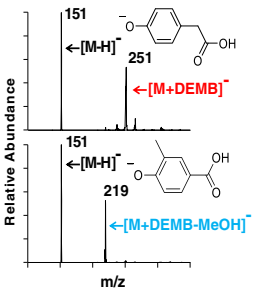

Abstract. Conversion of lignin into smaller molecules provides a promising alternate and sustainable source for the valuable chemicals currently derived from crude oil. Better understanding of the chemical composition of the resulting product mixtures is essential for the optimization of such conversion processes. However, these mixtures are complex and contain isomeric molecules with a wide variety of functionalities, which makes their characterization challenging. Tandem mass spectrometry based on ion–molecule reactions has proven to be a powerful tool in functional group identification and isomer differentiation for previously unknown compounds. This study demonstrates that the identification of the phenol functionality, the most commonly observed functionality in lignin degradation products, can be achieved via ion–molecule reactions between diethylmethoxyborane (DEMB) and the deprotonated analyte in the absence of strongly electron-withdrawing substituents in the *ortho*- and *para*-positions. Either a stable DEMB adduct or an adduct that has lost a methanol molecule (DEMB adduct-MeOH) is formed for these ions. Deprotonated phenols with an adjacent phenol or hydroxymethyl functionality or a conjugated carboxylic acid functionality can be identified based on the formation of DEMB adduct-MeOH. Deprotonated compounds not containing the phenol functionality and phenols containing an electron-withdrawing *ortho*- or *para*-substituent were found to be unreactive toward diethylmethoxyborane. Hence, certain deprotonated isomeric compounds with phenol and carboxylic acid, aldehyde, carboxylic acid ester, or nitro functionalities can be differentiated via these reactions. The above mass spectrometry method was successfully coupled with high-performance liquid chromatography for the analysis of a complex biomass degradation mixture.

Keywords: Ion–molecule reactions, Lignin degradation products, Phenol functionality, Phenols

Received: 31 March 2016/Revised: 20 June 2016/Accepted: 21 June 2016/Published Online: 23 August 2016

Introduction

The pursuit of renewable and sustainable chemical resources for energy and chemicals currently derived from crude oil has motivated researchers in exploring the conversion of lignocellulosic biomass into fuels and chemicals [1–6]. An important component of lignocellulosic biomass is lignin, which can make up to 25% of whole lignocellulosic biomass [7]. Lignin is a heavily crosslinked biopolymer composed of phenolic units with diverse and complex structural motifs [8, 9]. Due to its high aromatic carbon content, researchers have focused on converting lignin into valuable aromatic chemicals [7–10]. However, the inherent complexity of lignin often leads to the production of very complex mixtures of molecules with a wide variety of functionalities. The analysis of such mixtures is a challenging task. Yet, chemical characterization of these product mixtures is essential for the optimization of the lignin degradation processes and further conversion of the products into valuable chemicals.

Tandem mass spectrometry has proven to be a powerful tool in the characterization of lignin degradation product mixtures. Negative ion mode electrospray ionization (ESI) with sodium

Electronic supplementary material The online version of this article (doi:10.1007/s13361-016-1442-9) contains supplementary material, which is available to authorized users.

Correspondence to: Hilkka I. Kenttämaa; *e-mail:* hilkka@purdue.edu

hydroxide dopant has been identified as the best ionization method for degraded lignin as it exclusively forms deprotonated molecules with no fragmentation for lignin model compounds [11]. Other ionization methods, such as positive ion mode ESI or atmospheric pressure chemical ionization (APCI), either cause extensive fragmentation or form multiple ion types for each compound [11]. When used in HPLC/tandem mass spectrometry experiments, negative ion mode ESI facilitates the analysis of complex lignin degradation product mixtures [12, 13]. Structural information for the ionized molecules can be obtained via multiple stages of ion isolation and collisionally activated dissociation (CAD) experiments [14]. However, isomeric ions can have similar CAD fragmentation patterns, making their differentiation challenging [12]. Therefore, new methods for structural elucidation of isomeric aromatic ions are needed.

Past studies have shown that ion–molecule reactions can be a powerful tool for structural elucidation of ionized analytes [15, 16]. Identification of functional groups can be achieved by using neutral reagents that exhibit specific reactivity towards ions with these functional groups [17–23]. However, most studies on functional group-specific ion–molecule reactions have focused on protonated analytes. Only in a few cases were deprotonated analytes examined [24–28], and to the best of our knowledge, no reagents have been developed for the identification of the phenol functionality. In this study, diethyl methoxyborane (DEMB) is explored as a reagent for the identification of the phenol functionality in deprotonated lignin-related analytes. DEMB is known to react with negative ions and has been shown to allow differentiation of isobaric ions (deprotonated phosphorus- and sulfocarbohydrates) [25].

Experimental

Chemicals

Diethylmethoxyborane (97%), phenol (99%), 2-ethoxyphenol (98%), 3-methoxyphenol (96%), 4-ethoxyphenol (99%), 2-methoxy-4-propylphenol (99%), isoeugenol (98%), methyl ferulate (99%), catechol (99%), resorcinol (99%), hydroquinone (99%), 2-hydroxybenzyl alcohol (99%), 3-hydroxybenzyl alcohol (99%), benzoic acid (99.5%), terephthalic acid (98%), phthalic acid (99.5%), 3-nitrophenol (99%), 4-nitrophenol (99%), 2-hydroxybenzaldehyde (98%), 3-hydroxybenzaldehyde (99%), 4-hydroxybenzaldehyde (98%), methyl 2-hydroxybenzoate (99%), methyl 3-hydroxybenzoate (99%), methyl 4-hydroxybenzoate (99%), 2-hydroxybenzoic acid (99%), 3-hydroxybenzoic acid (99%), 4-hydroxybenzoic acid (99%), 2-hydroxycinnamic acid (99%), 3-hydroxycinnamic acid (98%), 4-hydroxycinnamic acid (97%), 2-hydroxyphenacetic acid (97%), 3-hydroxy phenacetic acid (99%), 4-hydroxyphenacetic acid (98%), vanillic acid (97%), syringic acid (95%), sinapic acid (98%), 4-methoxybenzoic acid (99%), and 4-hydroxy-3-methylbenzoic acid (97%) were purchased from Sigma Aldrich (MO, USA) and used as received. Vanillin (99%) was purchased from Fisher Scientific (MA, USA) and used as received. Guaiacylglycerol guaiacyl ether (97%) was purchased from TCI America (OR, USA) and used as received. Lignin β-5 dimer was synthesized via a previously reported method [29]. Converted *Miscanthus* biomass was obtained via a previously published procedure [30].

Mass Spectrometry

All experiments were performed on a Thermo Scientific (MA, USA) linear quadrupole ion trap (LQIT) mass spectrometer equipped with an electrospray ionization (ESI) source operated in the negative ion mode. Sample solutions were prepared at a concentration of 1 mmol in 50/50 water/methanol (v/v) solution. Ten μL of 1 mM NaOH water solution were added into 5 mL of sample solution to facilitate the formation of deprotonated analyte molecules. The NaOH-doped sample solutions were injected into the ion source at a flow rate of 10 μL/min. The injected solutions were mixed via a T-connector with 50/50 water/methanol (v/v) at a flow rate of 100 μL/min to maintain stable spray current. Typical ESI conditions were: 3.5 kV spray voltage, 20 (arbitrary unit) sheath gas (N_2) flow, 10 (arbitrary unit) auxiliary gas (N_2) flow, and 2 (arbitrary unit) sweep gas (N_2) flow.

Ion–Molecule Reactions

Ion–molecule reactions between deprotonated analytes and DEMB were studied using an external reagent mixing manifold described previously [18, 31, 32]. DEMB was injected into the manifold by using a syringe drive at a flow rate of 10 μL/min and then diluted with helium at a flow rate of 500 mL/min. The manifold was heated to 70 °C for efficient evaporation of DEMB into helium. The DEMB-helium mixture was then directed into a variable leak valve that allowed part of the mixture gas to enter the ion trap at a flow rate of 2 mL/min while the excess was directed into waste. Analyte ions were isolated using an isolation window of 2 *m/z* and a q value of 0.25. The isolated ions were allowed to react with DEMB for 30–500 ms before being ejected for detection.

High Performance Liquid Chromatography

All HPLC separations were performed on a Surveyor Plus HPLC system consisting of a dcolumn. A nonlinear gradient of water (A) and acetonitrile (B) was used as follows: 0.00 min, 95% A and 5% B; 10.00 min, 95% A and 5% B; 30.00 min, 40% A and 60% B; 35.00 min, 5% A and 95%; 38.00 min, 5% A and 95% B; 38.50 min, 95% A and 5% B; 45.00 min, 95% A and 5% B. The flow rate of the mobile phase was kept at 500 μL/min. PDA detector was set at the wavelength of 254 nm.

HPLC eluents were mixed via a T-connector with 1% sodium hydroxide solution at a flow rate of 0.1 μL/min before entering the ESI source. ESI source conditions were set as: 3.5 kV spray voltage; 50 (arbitrary unit) sheath gas (N_2) flow, and 20 (arbitrary unit) auxiliary gas (N_2) flow.

Table 1. Ionic Products Formed Upon Reactions of Deprotonated Model Compounds with Diethylmethoxyborane (DEMB) for 200 ms

Analyte ion (m/z of $[M-H]^-$)	Ion structure	Products formed upon reactions with DEMB[a] (m/z)
phenol (91)		91+DEMB (191)
2-ethoxyphenol (137)		137+DEMB (237)
3-methoxyphenol (137)	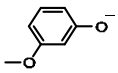	123+DEMB (223)
4-ethoxyphenol (123)	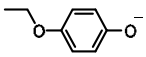	137+DEMB (237)
2-methoxy-4-propylphenol (165)	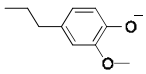	165+DEMB (265)
isoeugenol (163)	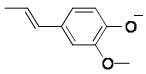	163+DEMB (263)
methyl ferulate (207)	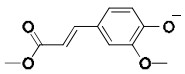	207+DEMB (307)
catechol (109)		109+DEMB-MeOH (177)
resorcinol (109)	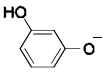	109+DEMB (209)
hydroquinone (109)	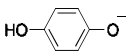	109+DEMB (209)
2-hydroxybenzyl alcohol (123)	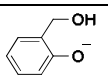	123+DEMB-MeOH (191)
3-hydroxybenzyl alcohol (123)	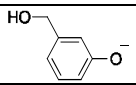	123+DEMB (223)
guaiacylglycerol guaiacyl ether (319)	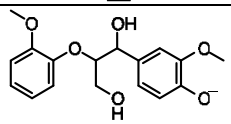	319+DEMB (419)
lignin β-5 dimer (325)	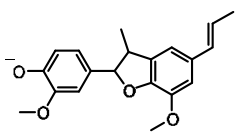	325+DEMB (425)
benzoic acid (121)		No products observed
terephthalic acid (165)	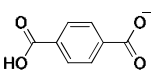	No products observed

[a] Only products with 5% or greater relative abundance reported. DEMB adduct are colored in red; DEMB adduct-MeOH are colored in blue

Computational Details

All density functional theory (DFT) calculations were performed using the Gaussian 09 software package [33]. Geometry optimizations were performed using the hybrid functional M06-2X [34] with the 6-31+G(d,p) basis set for potential surface calculations. All other geometries were optimized using 6-311++G(2d,p) basis set. Enthalpy values were obtained by calculating vibrational frequencies at the same level of theory at which they were optimized. Natural

bond orbital (NBO) analyses were performed at the M06-2X/6-311++G(2d,p) level of theory.

Results and Discussion

Multiple model compounds containing phenol, carboxylic acid, and other functionalities (Tables 1, 2, and 3) were ionized via negative ion mode ESI with NaOH as dopant. These compounds formed exclusively $[M - H]^-$ upon ionization. The deprotonated analytes were allowed to react with diethylmethoxyborane (DEMB) in order to explore whether it provides a useful reagent for the identification of the phenol functionality in deprotonated lignin-related analytes. After obtaining promising results on model compounds, the method was used to identify phenols in a catalytically converted biomass sample containing multiple phenolic compounds.

Formation of a DEMB Adduct for Deprotonated Phenols

Upon reactions with DEMB, deprotonated phenol and most deprotonated substituted phenols (Tables 1, 2, and 3) formed a DEMB adduct ion ($[M - H + DEMB]^-$) that has 100 units greater *m/z*-value than the analyte ion. The substituents include alkyl, alkenyl, hydroxymethyl, alkoxy, phenol (Table 1), nitro, aldehyde, carboxylic acid ester (Table 2), and carboxylic acid (Table 3). The boron-containing adduct can be easily identified by the characteristic boron isotope distribution (100% ^{11}B to 20% ^{10}B). Larger model compounds (i.e., two lignin dimers with β-O-

Table 2. Ionic Products Formed Upon Reactions of Deprotonated Phenol and Its Derivatives Containing Electron-Withdrawing Substituents with DEMB for 200 ms, Calculated NBO Charges of the Deprotonated Phenols at the Phenoxide Oxygen, and Calculated Energy Differences Between the Reactants and Their Products

Analyte ion (m/z of $[M-H]^-$)	Ion structure	Products formed upon reactions with DEMB[a] (m/z)	Calculated NBO charge[b]	Energy difference (kcal/mol)[d]
phenol (91)		91+DEMB (191)	-0.808[c]	-34.2
vanillin (151)	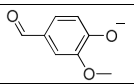	No products observed	-0.721[c]	-25.1
3-nitrophenol (138)	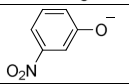	138+DEMB (238)	-0.782[c]	-28.8
4-nitrophenol (138)	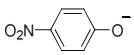	No products observed	-0.726[c]	-23.4
2-hydroxybenzaldehyde (121)		121+DEMB (221) minor	-0.766[c]	-27.3
3-hydroxybenzaldehyde (121)	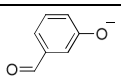	121+DEMB (221)	-0.793[c]	-31.0
4-hydroxybenzaldehyde (121)	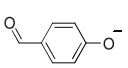	No products observed	-0.743[c]	-26.4
methyl 2-hydroxybenzoate (151)	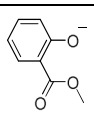	151+DEMB (251) minor	-0.724[c]	-27.6
methyl 3-hydroxybenzoate (151)	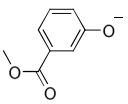	151+DEMB (251)	-0.798[c]	-31.9
methyl 4-hydroxybenzoate (151)	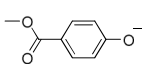	151+DEMB (251) minor	-0.752[c]	-27.2

[a] Products with 5% or greater relative abundance are colored in red. Products with relative abundance between 0.1% and 5% are considered to be minor
[b] NBO = natural bond orbital. Calculated at M06-2X/6-311G++(2d,p)
[c] Charge on the phenoxide oxygen atom
[d] Relative energy difference in enthalpy between product ion and separated reactants. Calculated at M06-2X/6-311G++(2d,p) level of theory

4 and β-5 linkages) also exclusively produced DEMB adducts (Table 1). However, deprotonated compounds not containing the phenol functionality, such as deprotonated benzoic acid, showed no reactivity towards DEMB (Table 1). Based on the above results and the results discussed below, the formation of a DEMB adduct is unique to deprotonated analytes with the phenol functionality. However, not all phenolic compounds form this adduct.

In contrast to the phenolic compounds discussed above, DEMB adduct formation was not observed for deprotonated vanillin (Table 2) that contains a phenol functionality as well as an electron-withdrawing aldehyde functional group. This observation led to further examination of the effects of electron-withdrawing substituents (aldehyde, nitro, and carboxylic acid ester) in the analyte ion on its reactivity toward DEMB (Table 2). Deprotonated phenols with an electron-withdrawing substituent at the *ortho*- or *para*-position were found to exhibit no reactivity towards DEMB, whereas the *meta*-substituted isomers formed the DEMB adduct ion (Table 2). An explanation for this behavior was sought by quantum chemical calculations.

Table 3. Ionic Products Formed upon Reactions of Deprotonated Model Compounds Containing a Phenol and a Carboxylic Acid Functional Group with DEMB for 200 ms

Analyte ion (m/z of $[M-H]^-$)	**Structure**	**Products formed upon reactions with DEMB[a] (m/z)**
2-hydroxybenzoic acid (137)		No products observed
3-hydroxybenzoic acid (137)	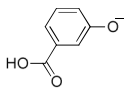	137+DEMB (251)
4-hydroxybenzoic acid (137)	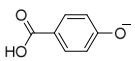	137+DEMB-MeOH (177)
2-hydroxycinnamic acid (137)	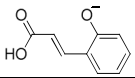	137+DEMB-MeOH (177)
3-hydroxycinnamic acid (137)	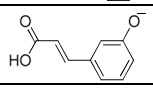	137+DEMB (251)
4-hydroxycinnamic acid (137)	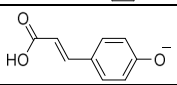	137+DEMB-MeOH (177)
2-hydroxyphenacetic acid (151)	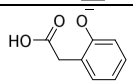	No products observed
3-hydroxyphenacetic acid (151)	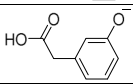	151+DEMB (251)
4-hydroxyphenacetic acid (151)	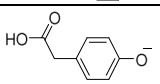	151+DEMB (251)
vanillic acid (16)	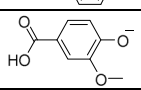	167+DEMB-MeOH (235)
syringic acid (197)	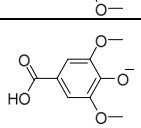	197+DEMB-MeOH (265)
sinapic acid (223)	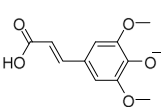	223+DEMB-MeOH (291)

[a]Only products with 5% or greater relative abundance are reported. DEMB adduct is colored in red, DEMB adduct-MeOH is colored in blue

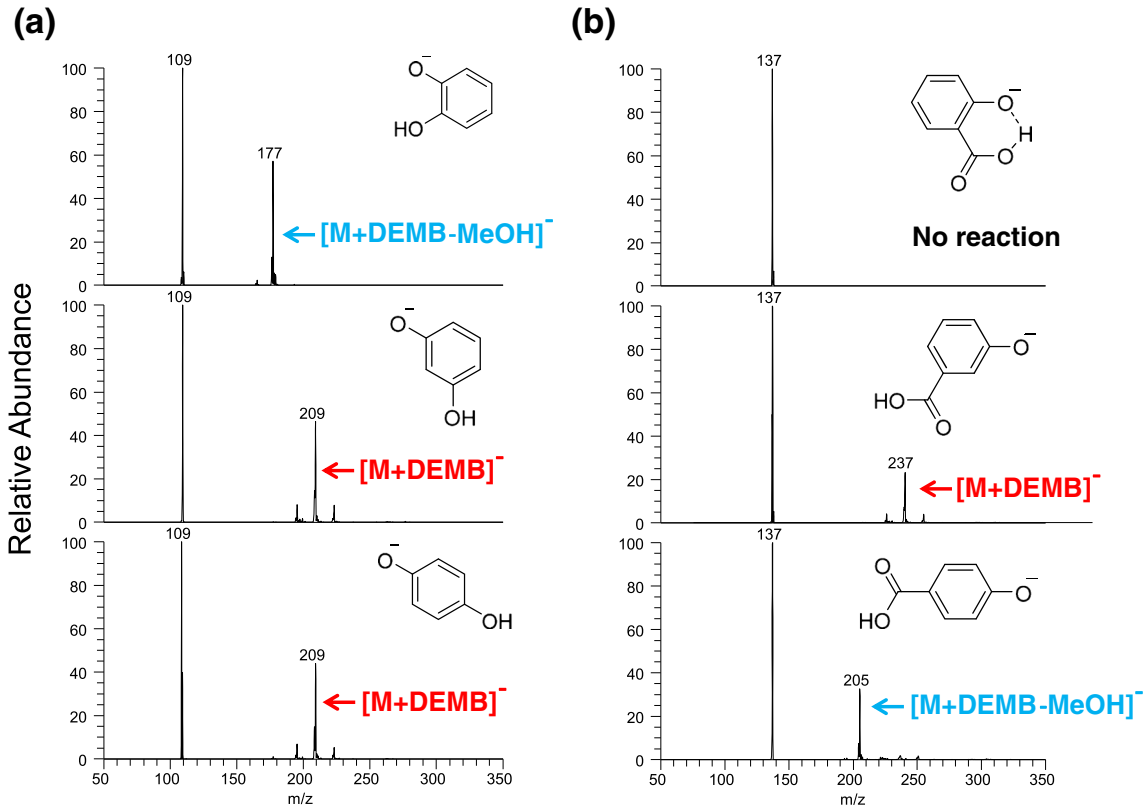

Figure 1. (**a**) Tandem mass spectra measured after reactions of (top) deprotonated catechol, (middle) deprotonated resorcinol, and (bottom) deprotonated hydroquinone with DEMB for 200 ms. (**b**) Tandem mass spectra measured after reactions of (top) deprotonated 2-hydroxybenzoic acid, (middle) deprotonated 3-hydroxybenzoic acid, and (bottom) deprotonated 4-hydroxybenzoic acid with DEMB for 200 ms

Calculations based on density functional theory showed that the NBO electron density on the phenoxide oxygen atom in deprotonated phenols is reduced in the presence of an *ortho*- or *para*-positioned electron-withdrawing substituent compared with *meta*-substituted phenols (Table 2), making them weaker nucleophiles. For example, the *meta*-substituted 3-hydroxybenzaldehyde has a NBO charge density of –0.793 on its phenoxide oxygen (formation of a stable DEMB adduct was observed) whereas its isomer, the *para*-substituted 4-hydroxybenzaldehyde, has a lower NBO charge density of –0.743 (no reactivity toward DEMB was observed). The *ortho*-substituted 2-hydroxybenzaldehyde has a NBO charge of –0.766 that falls between 3-hydroxy

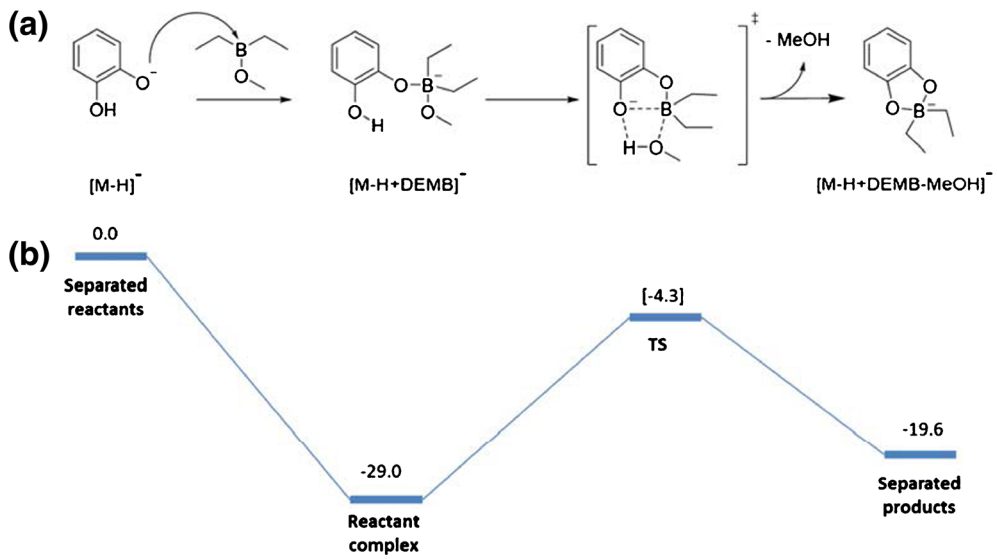

Figure 2. (**a**) Proposed mechanism and (**b**) calculated potential energy surface (enthalpy in kcal/mol) for the formation of a DEMB adduct that has lost methanol upon reactions between deprotonated catechol and DEMB (M06-2X/6-31+G(d,p) level of theory)

benzylaldehyde and 4-hydroxybenzyaldehyde (a minor DEMB adduct was observed). The above results show that a larger charge density on the phenoxide oxygen correlates with higher reactivity towards DEMB.

However, based on calculations, all the phenols form a low-energy covalently bound adduct with DEMB (Table 2). In the gas phase, these adducts are not stable toward dissociation back to reactants unless they are stabilized either by emission of IR light or by collisions with the helium buffer gas. The lower the energy of the adduct, the longer its lifetime, and the more likely it is that it gets stabilized via one of these processes. Indeed, the energy of the covalent DEMB adducts relative to the separated reactants (Table 2) was calculated to be greatest (from –29 down to –34 kcal/mol) for those ions that formed an abundant stable adduct as a final product, slightly less for those that formed a minor adduct (–27 kcal/mol) and even less for those that did not form a stable adduct (from –23 down to –26 kcal/mol). This likely explains the selectivity for stable DEMB adduct formation for different deprotonated phenols.

Formation of DEMB Adduct-MeOH

When deprotonated catechol (containing two adjacent phenol functionalities) was allowed to react with DEMB, it did not form a stable DEMB adduct but instead a DEMB adduct that had lost methanol ($[M - H + DEMB - MeOH]^-$) with 68 units greater *m*/*z*-value than the analyte ion (Table 1, Figure 1a). Formation of this type of product ion was not observed for the isomeric resorcinol or hydroquinone, which both formed a stable DEMB adduct instead (Table 1; Figure 1a). Exclusive formation of DEMB adduct-MeOH was also observed for deprotonated 2-hydroxybenzyl alcohol but not for the isomeric deprotonated 3-hydroxybenzyl alcohol, the hydroxyl and phenol groups of which are further away from each other (Table 1). These observations suggest that an additional phenol or hydroxyl functionality in close proximity to the deprotonated

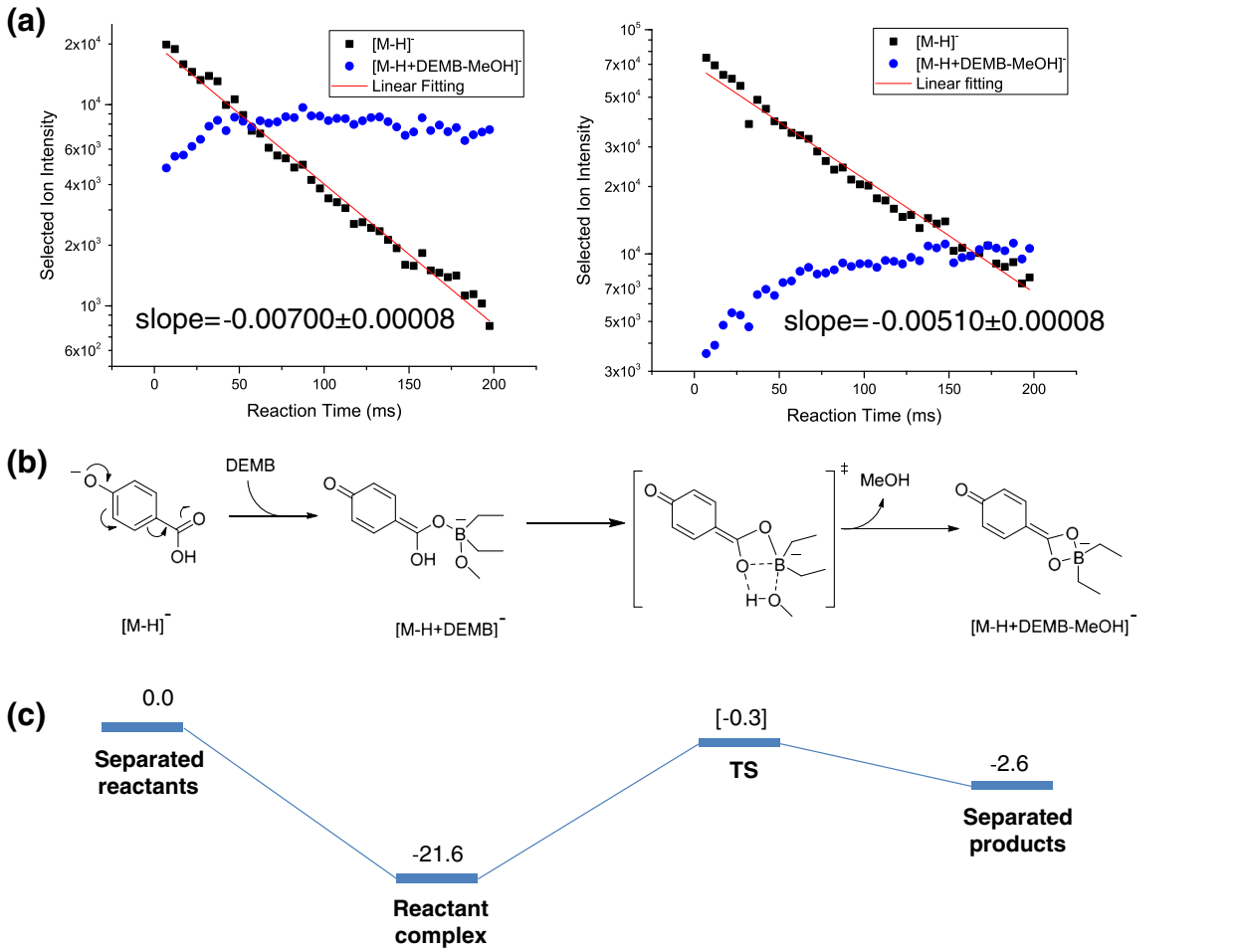

Figure 3. (**a**) Logarithm of the abundances of deprotonated 4-hydroxybenzoic acid (black symbols) and DEMB adduct-MeOH product ion (blue symbols) plotted as a function of reaction time for the reaction between DEMB and deprotonated 4-hydroxybenzoic acid generated using NaOH doped water solution (left) and acetonitrile solution (right). (**b**) Mechanism proposed for the formation of DEMB adduct that has lost methanol. (**c**) Calculated potential energy surface (enthalpies in kcal/mol) for the formation of DEMB adduct-MeOH (M06-2X/6-31+G(d,p) level of theory)

phenol group is critical for the formation of DEMB adduct-MeOH. The potential energy surface for the proposed mechanism, calculated via density functional theory, is shown in Figure 2 for catechol (CAD mass spectrum of the product ion is shown in Supplementary Table S1, Supporting Information).

Formation of DEMB adduct-MeOH was also observed for certain deprotonated phenols with carboxylic acid functionalities. When regioisomers of deprotonated hydroxycinnamic acid, hydroxyphenylacetic acid, and hydroxybenzoic acid were allowed to react with DEMB (Table 3), DEMB adduct-MeOH was observed for 4-hydroxybenzoic acid, 2-hydroxycinnamic acid, and 4-hydroxycinnamic acid, the phenol and carboxylic acid functionalities of which are conjugated. All other ions either only formed a DEMB adduct or were unreactive. The lack of products for 2-hydroxyphenylacetic acid and 2-hydroxybenzoic acid can be explained by the presence of strong intramolecular hydrogen bonding in their deprotonated forms (Figure 1b), which reduces their nucleophilicity. For the ions that formed DEMB adduct-MeOH, such as 4-hydroxybenzoic acid, the originally proposed mechanism (Figure 2) is no longer applicable since the distance between the carboxylic acid and phenol functionalities is too great. Therefore, a different mechanism must be involved.

One issue that must be considered here is that hydroxybenzoic acids have two possible deprotonation sites. If the benzoic acid moiety is exclusively deprotonated in some of them, one would expect no reactivity toward DEMB, based on the above results. Literature studies have shown that experimental conditions can influence the site of deprotonation of 4-hydroxybenzoic acid upon ESI [35, 36]. After some controversy on which is the preferred site of deprotonation in different solvent systems, the generally agreed upon conclusion appears to be that the phenoxide anion greatly dominates when using aprotic solvents (such as acetonitrile) while the carboxylate tautomer is also formed when using protic solvents (such as water) [35, 36]. In order to establish whether this applies to the present experiments utilizing ESI and protic solvents, the reactivity of DEMB toward 4-hydroxybenzoic acid deprotonated using different solvents was studied.

The abundances of 4-hydroxybenzoic acid deprotonated using an aprotic (acetonitrile) and protic solvent (water with 0.1% NaOH) and its DEMB adduct-MeOH product were measured as a function of reaction time. Ion–molecule reactions studied under the conditions utilized here follow pseudo-first order kinetics. Hence, a plot of the logarithm of the reactant ion's relative abundance versus reaction time is a straight line with a negative slope equal to the rate constant multiplied by

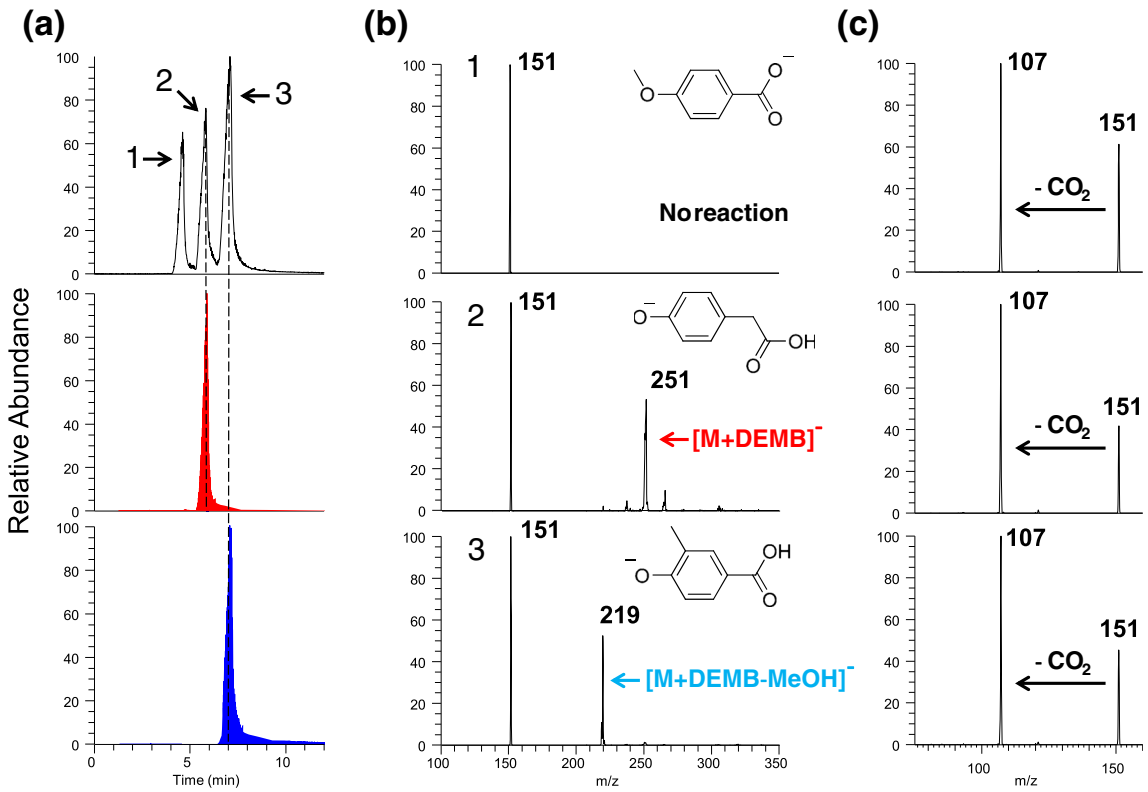

Figure 4. (**a**) (top) Total ion HPLC chromatogram measured for an equimolar mixture of 4-methoxybenzoic acid (1), 4-hydroxyphenylacetic acid (2), and 4-hydroxy-3-methylbenzoic acid (3). Selected ion HPLC chromatograms measured for all ions that formed DEMB adduct (middle), and DEMB adduct-MeOH (bottom) upon reaction with DEMB. (**b**) MS^2 spectra measured after reaction of deprotonated 4-methoxybenzoic acid (top), deprotonated 4-hydroxyphenacetic acid (middle), and deprotonated 4-hydroxy-3-methylbenzoic acid (bottom) with DEMB for 200 ms. (**c**) CAD MS^2 spectra measured for deprotonated 4-methoxybenzoic acid (top), deprotonated 4-hydroxyphenacetic acid (middle), and deprotonated 4-hydroxy-3-methylbenzoic acid (bottom) after a separate HPLC run followed by ionization, ion isolation and CAD

DEMB concentration. With the concentration of DEMB staying constant under the conditions employed here (the concentration of reactant ions is substantially smaller than the concentration of the reagent molecules), the rate constant is proportional to the value of the negative slope, which is larger (0.007 versus 0.005) when the reactant ions were generated using acetonitrile (Figure 3a). This finding is in agreement with the literature results discussed above that acetonitrile is expected to produce more phenoxide ions, whereas water doped with NaOH should produce more carboxylate anions (about 40% relative to the phenoxide ions) [35]. However, since both ion populations are reactive toward DEMB, phenoxide ions exist in both. Hence, exclusive deprotonation of the carboxylic acid moiety is unlikely. This finding is in agreement with the CAD mass spectra measured for 4-hydroxybenzoic acid deprotonated using the aprotic and protic solvent systems and the potential energy surfaces calculated for these reactions (Supplementary Figures S1 and S2). CO_2 loss from the phenoxide ion is calculated to be more energetically favorable than from the carboxylate ion (Supplementary Figure S1). Indeed, the ions generated from acetonitrile solution fragment more readily by CO_2 loss than the ions generated from water/NaOH solution (Supplementary Figure S2), suggesting that more phenoxide ions had been formed in the acetonitrile solution.

Based on the findings above, a new mechanism is proposed for the formation of DEMB adduct-MeOH (Figure 3b) for compounds with conjugated carboxylic acid and phenol functionalities, such as 4-hydroxybenzoic acid. In these deprotonated molecules, the charge on the deprotonated phenol moiety can resonate onto the carboxylic acid oxygen, which enables nucleophilic attack by the carboxylic acid moiety at the boron atom in DEMB. After addition, the carboxylic acid moiety can donate a proton to a methoxy group to eliminate methanol. Potential energy surface calculated for the proposed mechanism shows a low barrier of –0.3 kcal/mol for DEMB adduct-MeOH formation for the reaction between deprotonated 4-hydroxybenzoic acid and DEMB (Figure 3c; CAD mass spectrum of the product ion is shown in Supplementary Table S1 and proposed fragmentation mechanism in Supplementary Scheme S1).

DEMB Ion–Molecule Reactions Coupled with HPLC

The formation of a DEMB adduct or DEMB adduct-MeOH is fast. At 200 ms reaction time, the relative abundances of DEMB adduct ions with respect to analyte ions are greater than 20% for all model compounds that exhibit reactivity towards

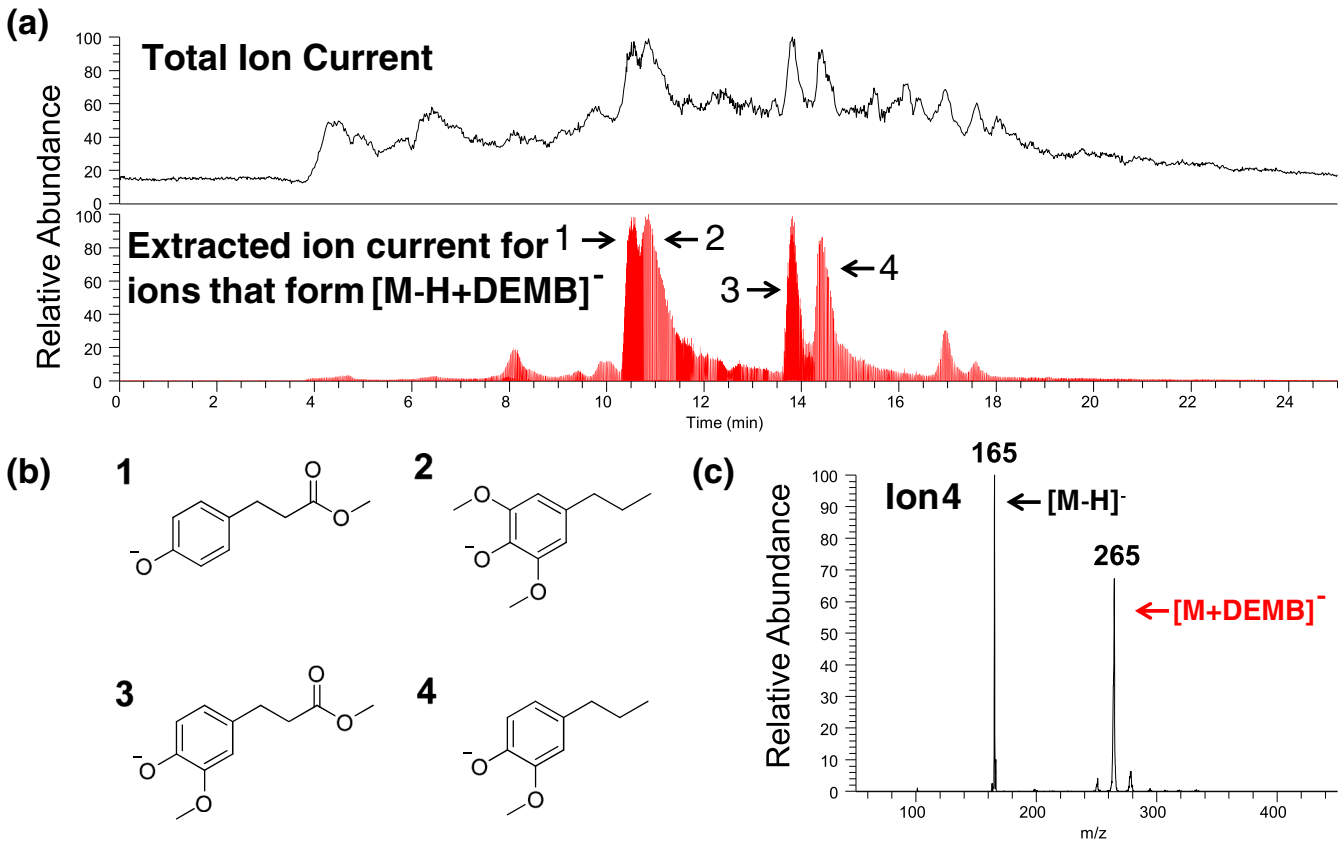

Figure 5. (**a**) (top) Total ion current HPLC chromatogram for a mixture obtained via catalytic conversion of *Miscanthus* biomass. (bottom) Selected ion HPLC chromatogram for all ions that form a DEMB adduct. (**b**) Structures of the four major phenols that were identified in the mixture. (**c**) MS^2 spectrum measured after isolation of ion **4** (*m/z* 165) and reaction with DEMB for 200 ms

DEMB. Thus, this reaction should be compatible with chromatographic time scale. In order to test this hypothesis, an equimolar mixture of three isomers, 4-methoxybenzoic acid, 4-hydroxyphenylacetic acid, and 4-hydroxy-3-methylbenzoic acid, was subjected to HPLC/tandem mass spectrometric analysis (Figure 4a). The compounds were eluted using a gradient consisting of water and acetonitrile, deprotonated via ESI as they eluted from the column, and allowed to react with DEMB for 200 ms in the ion trap. Typically, about 40 such MS experiments were performed for each HPLC peak. Due to the lack of a phenol functional group, deprotonated 4-methoxybenzoic acid showed no reactivity toward DEMB (Figure 4b). Deprotonated 4-hydroxy-3-methylbenzoic acid that contains both a phenol functional group and a conjugated carboxylic acid functional group formed DEMB adduct-MeOH, whereas deprotonated 4-hydroxyphenacetic acid formed DEMB adduct (Figure 4b). Hence, these three isomers can be differentiated using this approach. It is notable that these isomers cannot be differentiated when using conventional HPLC/MS^2 analysis based on CAD, as all three ionized isomeric compounds undergo the same fragmentations upon CAD (Figure 4c).

Once coupled with HPLC, the above approach can be used for rapid screening of mixtures for the presence of phenol-containing compound. This was demonstrated by the analysis of a product mixture obtained by catalytic conversion of *Miscanthus* biomass (Figure 5). Using the same water/acetonitrile gradient, HPLC eluates were ionized by negative ion mode ESI and the most abundant ion formed for each eluate was isolated and allowed to react with DEMB for 200 ms in the ion trap. The complexity of the product mixture is demonstrated by the total ion current chromatograph shown in Figure 5a. However, by monitoring ions that produce an ion with 100 units greater *m*/*z* value, an extracted ion chromatogram can be obtained that represents compounds with the phenol functionality (Figure 5a). No DEMB adduct-MeOH product ions were observed, indicating the absence of phenols with adjacent hydroxyl or conjugated carboxylic acid functionalities. For the product mixture studied, four major phenols were identified. Their structures were elucidated via CAD of their deprotonated forms and comparison to CAD of model compounds (Figure 5b) [30].

Conclusions

A tandem mass spectrometry method is presented for the selective detection of the phenol functionality in di- and polyfunctional analytes related to lignin. The method is based on gas-phase ion–molecule reactions of the deprotonated analytes with DEMB. All deprotonated phenol model compounds form stable DEMB adduct ions ($[M - H + DEMB]^-$) or DEMB adduct ions that have lost a methanol molecule ($[M - H + DEMB\text{-}MeOH]^-$) except for the ones with a strong electron withdrawing substituent in the *ortho*- or *para*-position. Deprotonated phenols with an adjacent phenol or hydroxymethyl group and those with a conjugated carboxylic acid group can be identified based on the formation of DEMB adduct-MeOH, although this product ion is formed via different mechanisms for these two types of analytes. Deprotonated compounds with no phenol functionalities and phenols with an electron-withdrawing substituent in the *ortho*- or *para*-position were unreactive toward DEMB. By coupling the above technique with HPLC, an entire class of analytes can be identified in complex mixtures by using a single HPLC run. A catalytically converted *Miscanthus* biomass sample was analyzed to demonstrate the potential of tandem mass spectrometry based on ion–molecule reactions as a high-throughput screening tool for lignin degradation product mixtures.

Acknowledgments

This material is based upon work supported as part of the Center for Direct Catalytic Conversion of Biomass to Biofuels (C3Bio), an Energy Frontier Research Center funded by the U.S. Department of Energy, Office of Basic Energy Sciences, award number DE-SC0000997.

References

1. Service, R.F.: Battle for the barrel. Science **339**, 1374–1379 (2013)
2. Hamelinck, C.N., van Hooijdonk, G., Faaij, A.P.: Ethanol from lignocellulosic biomass: techno-economic performance in short-, middle- and long-term. Biomass Bioenerg. **28**, 384–410 (2005)
3. Hisano, H., Nandakumar, R., Wang, Z.-Y.: Genetic modification of lignin biosynthesis for improved biofuel production. Vitro Cell. Dev. Biol. Plant **45**, 306–313 (2009)
4. Chang, M.C.Y.: Harnessing energy from plant biomass. Curr. Opin. Chem. Biol. **11**, 677–684 (2007)
5. Ragauskas, A.J., Williams, C.K., Davison, B.H., Britovsek, G., Cairney, J., Eckert, C.A., Frederick, W.J., Hallett, J.P., Leak, D.J., Liotta, C.L., Mielenz, J.R., Murphy, R., Templer, R., Tschaplinski, T.: The path forward for biofuels and biomaterials. Science **311**, 484–489 (2006)
6. Weng, J.-K., Li, X., Bonawitz, N.D., Chapple, C.: Emerging strategies of lignin engineering and degradation for cellulosic biofuel production. Curr. Opin. Biotechnol. **19**, 166–172 (2008)
7. Calvo-Flores, F.G., Dobado, J.A.: Lignin as renewable raw material. ChemSusChem. **3**, 1227–1235 (2010)
8. Azadi, P., Inderwildi, O.R., Farnood, R., King, D.A.: Liquid fuels, hydrogen, and chemicals from lignin: a critical review. Renew. Sustain. Energy Rev. **21**, 506–523 (2013)
9. Zakzeski, J., Bruijnincx, P.C.A., Jongerius, A.L., Weckhuysen, B.M.: The catalytic valorization of lignin for the production of renewable chemicals. Chem. Rev. **110**, 3552–3599 (2010)
10. Parsell, T., Yohe, S., Degenstein, J., Jarrell, T., Klein, I., Gencer, E., Hewetson, B., Hurt, M., Kim, J.I., Choudhari, H., Saha, B., Meilan, R., Mosier, N., Ribeiro, F., Delgass, W.N., Chapple, C., Kenttämaa, H.I., Agrawal, R., Abu-Omar, M.M.: A synergistic biorefinery based on catalytic conversion of lignin prior to cellulose starting from lignocellulosic biomass. Green Chem. **17**, 1492–1499 (2015)
11. Haupert, L.J., Owen, B.C., Marcum, C.L., Jarrell, T.M., Pulliam, C.J., Amundson, L.M., Narra, P., Aqueel, M.S., Parsell, T.H., Abu-Omar, M.M., Kenttämaa, H.I.: Characterization of model compounds of processed lignin and the lignome by using atmospheric pressure ionization tandem mass spectrometry. Fuel **95**, 634–641 (2012)
12. Jarrell, T.M., Marcum, C.L., Sheng, H., Owen, B.C., O'Lenick, C.J., Maraun, H., Bozell, J.J., Kenttämaa, H.I.: Characterization of organosolv switchgrass lignin by using high performance liquid chromatography/high resolution tandem mass spectrometry using hydroxide-doped negative-ion mode electrospray ionization. Green Chem. **16**, 2713–2727 (2014)
13. Owen, B.C., Haupert, L.J., Jarrell, T.M., Marcum, C.L., Parsell, T.H., Abu-Omar, M.M., Bozell, J.J., Black, S.K., Kenttämaa, H.I.: High-performance

liquid chromatography/high-resolution multiple stage tandem mass spectrometry using negative-ion-mode hydroxide-doped electrospray ionization for the characterization of lignin degradation products. Anal. Chem. **84**, 6000–6007 (2012)
14. Amundson, L.M., Eismin, R.J., Reece, J.N., Fu, M., Habicht, S.C., Mossman, A.B., Shea, R.C., Kenttämaa, H.I.: Identification and counting of oxygen functionalities in aromatic analytes related to lignin by using negative-mode electrospray ionization and multiple collision-activated dissociation steps. Energy Fuels **25**, 3212–3222 (2011)
15. Brodbelt, J.S.: Analytical applications of ion–molecule reactions. Mass Spectrom. Rev. **16**, 91–110 (1997)
16. Eberlin, M.N.: Structurally diagnostic ion/molecule reactions: class and functional-group identification by mass spectrometry. J. Mass Spectrom. **41**, 141–156 (2006)
17. Somuramasami, J., Winger, B.E., Gillespie, T.A., Kenttämaa, H.I.: Identification and counting of carbonyl and hydroxyl functionalities in protonated bifunctional analytes by using solution derivatization prior to mass spectrometric analysis via ion–molecule reactions. J. Am. Soc. Mass Spectrom. **21**, 773–784 (2010)
18. Habicht, S.C., Vinueza, N.R., Archibold, E.F., Duan, P., Kenttämaa, H.I.: Identification of the carboxylic acid functionality by using electrospray ionization and ion-molecule reactions in a modified linear quadrupole ion trap mass spectrometer. Anal. Chem. **80**, 3416–3421 (2008)
19. Sheng, H., Williams, P.E., Tang, W., Riedeman, J.S., Zhang, M., Kenttämaa, H.I.: Identification of the sulfone functionality in protonated analytes via ion/molecule reactions in a linear quadrupole ion trap mass spectrometer. J. Org. Chem. **79**, 2883–2889 (2014)
20. Watkins, M.A., Winger, B.E., Shea, R.C., Kenttämaa, H.I.: Ion−molecule reactions for the characterization of polyols and polyol mixtures by ESI/FT-ICR mass spectrometry. Anal. Chem. **77**, 1385–1392 (2005)
21. Fu, M., Duan, P., Gao, J., Kenttämaa, H.I.: Ion–molecule reactions for the differentiation of primary, secondary and tertiary hydroxyl functionalities in protonated analytes in a tandem mass spectrometer. Analyst **137**, 5720 (2012)
22. Sheng, H., Tang, W., Yerabolu, R., Kong, J.Y., Williams, P.E., Zhang, M., Kenttämaa, H.I.: Mass spectrometric identification of the N-monosubstituted N-hydroxylamino functionality in protonated analytes via ion/molecule reactions in tandem mass spectrometry. Rapid Commun. Mass Spectrom. **29**, 730–734 (2015)
23. Fu, M., Duan, P., Li, S., Habicht, S.C., Pinkston, D.S., Vinueza, N.R., Kenttämaa, H.I.: Regioselective ion–molecule reactions for the mass spectrometric differentiation of protonated isomeric aromatic diamines. Analyst **133**, 452 (2008)
24. Piatkivskyi, A., Pyatkivskyy, Y., Ryzhov, V.: Evaluation of various silicon- and boron-containing compounds for the detection of phosphorylation in peptides via gas-phase ion–molecule reactions. Eur. J. Mass Spectrom. Chichester Engl. **20**, 337–344 (2014)
25. Piatkivskyi, A., Pyatkivskyy, Y., Hurt, M., Ryzhov, V.: Utilization of gas-phase ion–molecule reactions for differentiation between phospho- and sulfocarbohydrates. Eur. J. Mass Spectrom. **20**, 177 (2014)
26. Gronert, S., O'Hair, R.A.J.: Gas phase reactions of trimethyl borate with phosphates and their non-covalent complexes†. J. Am. Soc. Mass Spectrom. **13**, 1088–1098 (2002)
27. Gao, H., Petzold, C.J., Leavell, M.D., Leary, J.A.: Investigation of ion/molecule reactions as a quantification method for phosphorylated positional isomers: an FT-ICR approach. J. Am. Soc. Mass Spectrom. **14**, 916–924 (2003)
28. Leavell, M.D., Kruppa, G.H., Leary, J.A.: Analysis of phosphate position in hexose monosaccharides using ion−molecule reactions and SORI-CID on an FT-ICR mass spectrometer. Anal. Chem. **74**, 2608–2611 (2002)
29. Forsythe, W.G., Garrett, M.D., Hardacre, C., Nieuwenhuyzen, M., Sheldrake, G.N.: An efficient and flexible synthesis of model lignin oligomers. Green Chem. **15**, 3031–3038 (2013)
30. Luo, H., Klein, I.M., Jiang, Y., Zhu, H., Liu, B., Kenttamaa, H.I., Abu-Omar, M.M.: Total utilization of *Miscanthus* biomass, lignin and carbohydrates, using earth abundant nickel catalyst. ACS Sustain. Chem. Eng. (2016)
31. Gronert, S.: Quadrupole ion trap studies of fundamental organic reactions. Mass Spectrom. Rev. **24**, 100–120 (2005)
32. Gronert, S.: Estimation of effective ion temperatures in a quadrupole ion trap. J. Am. Soc. Mass Spectrom. **9**, 845–848 (1998)
33. Frisch, M.J., Trucks, G.W., Schlegel, H.B., Scuseria, G.E., Robb, M.A., Cheeseman, J.R., Scalmani, G., Barone, V., Mennucci, B., Petersson, G.A., Nakatsuji, H., Caricato, M., Li, X., Hratchian, H.P., Izmaylov, A.F., Bloino, J., Zheng, G., Sonnenberg, J.L., Hada, M., Ehara, M., Toyota, K., Fukuda, R., Hasegawa, J., Ishida, M., Nakajima, T., Honda, Y., Kitao, O., Nakai, H., Vreven, T., Montgomery Jr., J.A., Peralta, J.E., Ogliaro, F., Bearpark, M.J., Heyd, J., Brothers, E.N., Kudin, K.N., Staroverov, V.N., Kobayashi, R., Normand, J., Raghavachari, K., Rendell, A.P., Burant, J.C., Iyengar, S.S., Tomasi, J., Cossi, M., Rega, N., Millam, N.J., Klene, M., Knox, J.E., Cross, J.B., Bakken, V., Adamo, C., Jaramillo, J., Gomperts, R., Stratmann, R.E., Yazyev, O., Austin, A.J., Cammi, R., Pomelli, C., Ochterski, J.W., Martin, R.L., Morokuma, K., Zakrzewski, V.G., Voth, G.A., Salvador, P., Dannenberg, J.J., Dapprich, S., Daniels, A.D., Farkas, Ö., Foresman, J.B., Ortiz, J.V., Cioslowski, J., Fox, D.J.: Gaussian 09. Gaussian, Inc.: Wallingford, CT, USA (2009)
34. Zhao, Y., Truhlar, D.G.: The M06 suite of density functionals for main group thermochemistry, thermochemical kinetics, noncovalent interactions, excited states, and transition elements: two new functionals and systematic testing of four M06-class functionals and 12 other functionals. Theor. Chem. Acc. **120**, 215–241 (2007)
35. Schröder, D., Buděšínský, M., Roithová, J.: Deprotonation of p-hydroxybenzoic acid: does electrospray ionization sample solution or gas-phase structures? J. Am. Chem. Soc. **134**, 15897–15905 (2012). **and references therein**
36. Steill, J.D., Oomens, J.: Gas-phase deprotonation of p-hydroxybenzoic acid investigated by IR spectroscopy: solution-phase structure is retained upon ESI. J. Am. Chem. Soc. **131**, 13570–13571 (2009). **and references therein**